Line shape of time-resolved four-wave mixing

M. Wegener and D. S. Chemla
AT&T Bell Laboratories, Holmdel, New Jersey 07733

S. Schmitt-Rink
AT&T Bell Laboratories, Murray Hill, New Jersey 07974

W. Schäfer
Forschungszentrum Jülich, Hochleistungsrechenzentrum, 5170 Jülich, Federal Republic of Germany
(Received 8 May 1990)

Time-resolved four-wave-mixing experiments are usually interpreted in terms of noninteracting two-level systems in order to obtain information on the polarization dephasing time T_2. Recent experiments involving excitonic resonances in semiconductor quantum wells (including results presented in this paper) show striking qualitative deviations from this simple picture. In particular, an exponential tail is observed at low excitation for negative time delays. At high excitation, the four-wave-mixing signal is found to evolve into two distinct temporal maxima. We demonstrate that the microscopic origin of this time dependence can be understood in terms of coherent exciton-exciton interactions. We show in fact that this behavior is more general and should be seen in numerous dense media where strong nonlinear interactions of polarizations occur. In addition to presenting rigorous numerical results, we analyze two simple situations in which such interactions exist: dielectric media with local-field effects and the anharmonic oscillator. We derive analytical expressions for their time-dependent four-wave-mixing response and discuss the physical origin of these new nonlinear-optical effects.

I. INTRODUCTION

In the density-matrix description of quantum-mechanical systems, the effects of random perturbations and damping are usually accounted for by introducing phenomenological relaxation terms in the equations of motion. In this approach the damping of the diagonal and off-diagonal terms of the density matrix are characterized by two types of time constants, T_1 and T_2, which describe, respectively, the lifetime of the populations of the levels and the loss of coherence of the transition amplitude between two such levels. This analysis is particularly simple in the case of two-level systems, the linear and nonlinear-optical response of which have been extensively investigated.[1,2] In general, the damping parameters T_1 and T_2 are extremely difficult to calculate and therefore they are deduced from experiments. Hence the importance of a correct procedure to deduce them from experimental data.

A very powerful and elegant method to study dephasing processes in the optical response is time-resolved four-wave mixing (FWM).[2] In this technique two pulsed laser beams with wave vectors $\mathbf{k}_1$ and $\mathbf{k}_2$ interfere in a sample to produce a diffracted beam in the direction $\mathbf{k}_3=2\mathbf{k}_2-\mathbf{k}_1$. The magnitude of the diffracted signal in the direction $\mathbf{k}_3$ is then recorded as a function of the time delay $T=t_2-t_1$ between a pulse of beam 2 and a pulse of beam 1 (Fig. 1). The experimental results are usually interpreted in terms of the pioneering work of Yajima and Taira,[3] who introduced a noninteracting two-level model to determine the polarization dephasing time T_2 during which the system has not experienced incoherent scattering.

In the context of semiconductor physics, important information on incoherent scattering of excitons by acoustic phonons, impurities, other excitons, and free electrons (e) and holes (h) has been obtained by time-resolved FWM experiments in GaAs quantum wells (QW's).[4] Quantum beats, which are a direct manifestation of coherence, have also been seen between closely spaced exciton levels in GaAs QW's.[5] Finally, even the extremely fast density-dependent scattering of free e and h among themselves has been measured in GaAs using ultrashort laser pulses.[6]

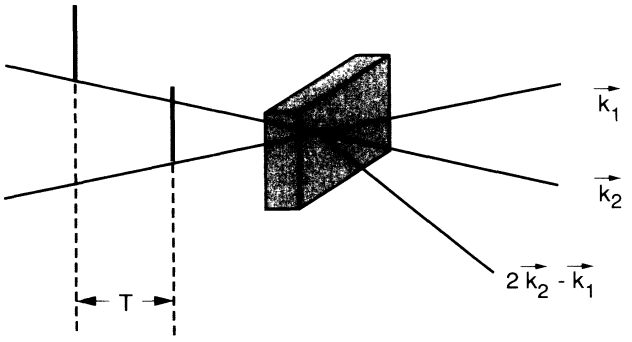

FIG. 1. Schematic of the geometry of four-wave mixing. In our notation, positive time delay T corresponds to pulse 1 preceding pulse 2.

The present paper addresses the general question of the validity of the noninteracting two-level model analysis for the case of dense media. It is organized as follows. In Sec. II we present experimental results on time-resolved FWM close to excitonic resonances in semiconductor QW's at low temperatures with ultrashort (140 fs) duration pulses. At high excitation, we find a time evolution of the FWM signal which qualitatively disagrees with an analysis based on noninteracting two-level systems. In Sec. III we summarize the quantum kinetic equations for interacting e and h in semiconductors and present numerical solutions of the complete set of equations to all orders for finite pulses. These are directly compared to our experiments. It is found that the Coulomb force produces nonlinearities that can be interpreted as due to coherent exciton-exciton interactions. These terms have previously been introduced in the context of the excitonic ac Stark effect.[7] They involve a direct coherent coupling of e-h pair amplitudes and populations via the Coulomb potential. As shown in Ref. 8, their signature in the time domain is qualitatively different from that of noninteracting two-level systems, for which the FWM signal solely originates from the coupling of the population to the applied field. At low density, exciton-exciton interactions result in a signal at negative time delays, $T<0$, which gradually evolves into a temporal profile with two distinct maxima as the density increases.[9] Since it seems that the origin of these effects is of quite general nature, they should also be seen in other situations where nonlinear couplings of polarizations or polarization and population exist. In order to demonstrate that this is indeed the case we consider, in Secs. IV and V, two situations that exhibit such couplings. In Sec. IV we discuss the case of interacting two-level systems in a dense medium where local-field effects are important and in Sec. V the case of a single anharmonic oscillator that can describe a molecule, for example. We find that for both cases very simple analytical models give a comprehensive phenomenological description of all the observed effects including inhomogeneous broadening. The models are simple and general enough to make the underlying physics transparent and point out experimental conditions where the same temporal profile should be observed in time-resolved FWM.

II. EXPERIMENTAL STUDIES OF TIME-RESOLVED FOUR-WAVE MIXING IN QUANTUM WELLS

The source of fs pulses in our experiment is a tunable, 140-fs full width at half maximum (FWHM) duration, additive-pulse mode-locked color-center laser, similar to that described in Ref. 10. The pulses are nearly transform limited. We split the beam into two beams with wave vectors $\mathbf{k}_1$ and $\mathbf{k}_2$ and intensity ratio $I_2/I_1=3$. The two beams are focused to one spot with a 7-cm focal length lens. We detect the diffracted beam in direction $\mathbf{k}_3=2\mathbf{k}_2-\mathbf{k}_1$ with a slow detector (cooled Ge), which thus measures the energy of the diffracted pulse. The geometry is illustrated in Fig. 1. The signal is measured as a function of the time delay T between the two pulses. Several experiments at various intensities are performed. The samples consist of multiple (20–60) layers with 200-Å $In_{1-x}Ga_xAs$ QW's and $In_{1-x}Al_xAs$ or InP barriers. One of the $In_{1-x}Ga_xAs/In_{1-x}Al_xAs$ samples is described in some detail in Ref. 11. For this rather large well width the heavy-hole and light-hole excitons are not resolved.[11] Furthermore, since the well material is a ternary compound, alloy disorder produces significant inhomogeneous broadening of the exciton line,[12] in addition to well-width fluctuations which are the main cause of broadening in binary QW's, such as GaAs QW's. For the FWM experiments the samples are held at fixed temperature 5 K→300 K, in a He-flow cryostat.

In Fig. 2 we show the sample absorption at 5 K (solid line). For exactly resonant excitation, we observe only symmetric FWM signals, indicating that in this case T_2 is shorter than our pulse. In this condition, however, we generate directly a significant amount of free e-h pairs because the bandwidth of the laser (10 meV) is larger than the exciton binding energy (≈4 meV). Therefore, in order to avoid this, we tune the laser below the exciton resonance. The spectrum of the fs laser for a detuning of 10 meV is also shown in Fig. 2. Typical results of time-dependent FWM signals are shown in Fig. 3 for low densities of excitons ($N\approx 5\times 10^9$ cm^{-2}) and various temperatures. T_2 is clearly resolved. In this regime, we find the decay time to be insensitive to the excitation density in a small range, i.e., when increasing or decreasing the incident laser intensity by a factor of 2. At 5 K the decay time is about 140 fs, which corresponds to $T_2\approx 550$ fs, assuming that the exciton line is inhomogeneously broadened. The $In_{1-x}Ga_xAs/InP$ sample has only a slightly longer dephasing time of $T_2\approx 700$ fs, whereas in a second $In_{1-x}Ga_xAs/In_{1-x}Al_xAs$ sample as well as in bulk $In_{1-x}Ga_xAs$ T_2 is below our resolution (dashed line in Fig. 3). Comparing this short T_2 to that measured in similar experiments in GaAS QW's,[4] we find a significantly shorter dephasing in the ternary system. Let

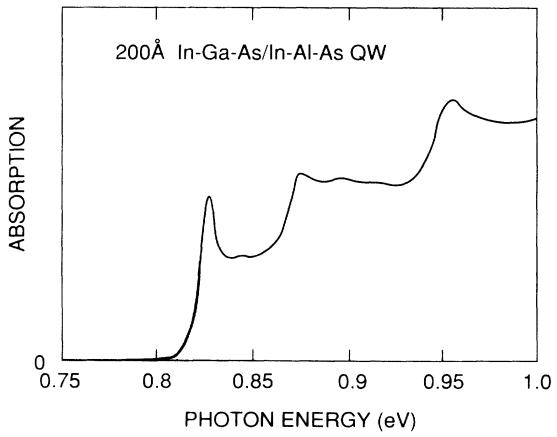

FIG. 2. Absorption spectrum of the 200-Å $In_{1-x}Ga_xAs/In_{1-x}Al_xAs$ multiple quantum well structure at 5 K. The spectrum of the additive-pulse mode-locked color-center laser for 10-meV detuning is also shown.

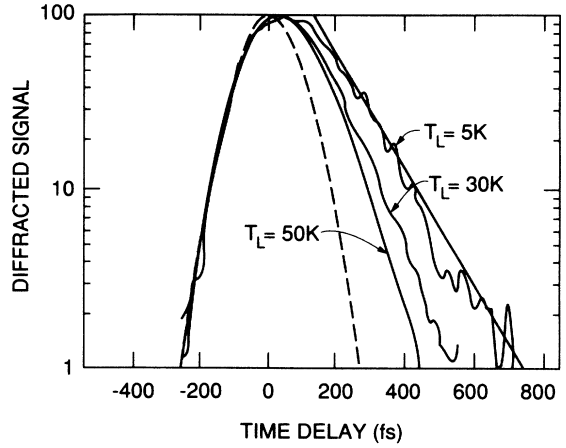

FIG. 3. Diffracted signal vs time delay for three different temperatures. The decay becomes faster as the thermal population of acoustic phonons rises. The decay constants are 140 (5), 100 (30), and 70 fs (50 K). The dashed line shows the time resolution of the experiment.

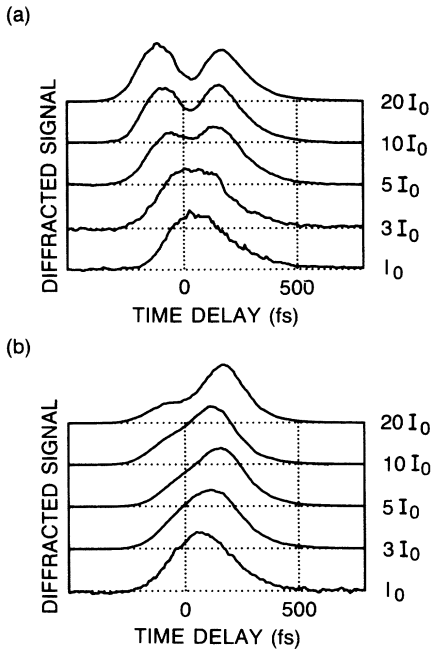

FIG. 4. Diffracted signal vs time delay for five different excitation intensities ($I_0 \approx 3$ MW cm^{-2}). (a) 10- and (b) 6-meV detuning.

us note that this is consistent with the fact that the oscillator strength of the excitonic transition as observed in the absorption spectrum is also lower than in GaAs. It is furthermore consistent with the fact that the recombination lifetime in $In_{1-x}Ga_xAs$ QW samples is typically of the order of several ns (sometimes up to 10 ns), as compared to a typical value of ≈ 1 ns for GaAs (500 ps for the sample in Ref. 4). All these results relate the short dephasing time to a small coherence volume of the exciton, which reduces its oscillator strength and thus increases the radiative lifetime.[13] This shorter dephasing of the excitons in the ternary system is most likely due to the additional scattering off local band gap fluctuations associated with alloy disorder.[12] We have presented independent indications of such an additional scattering process in a previous study of exciton ionization in this material system.[11] As the temperature is increased, T_2 decreases (Fig. 3), qualitatively reproducing the observation of Ref. 4 for GaAs QW's. This is easily understood in terms of scattering by acoustic phonons, the population of which increases with temperature.

In Figs. 4(a) and 4(b), we plot the FWM signals for 10- and 6-meV detuning, respectively, as the intensity of both beams is scaled up simultaneously from $I_0 = 3$ MW cm^{-2} to $20I_0$. For the highest intensities we estimate the exciton density to be of the order of $N \approx 10^{11}$ cm^{-2}, comparable to the saturation density of the exciton. As the incident intensity is increased, we observe the evolution of two different features. First the strength of the signal for negative time delays increases. Then the single-maximum temporal profile at low intensities gradually evolves into a line shape that exhibits two distinct maxima in time for 10-meV detuning and a strong asymmetry for 6-meV detuning. We verified that the signal in direction $2\mathbf{k}_1 - \mathbf{k}_2$ has the same time dependence for inverted time delay. For the 10-meV detuning experiment [Fig. 4(a)], the highest intensity $20I_0 \approx 60$ MW cm^{-2} corresponds to a regime of significant saturation of the resonance, and yet we still resolve a decay time of ≈ 80 fs for positive time delays. At this point the excitonic line has broadened due to the high exciton density. Assuming a homogeneous line yields $T_2 \approx 160$ fs. The fact that we can still resolve T_2 at a density where excitons are densely packed in real space is quite remarkable. For the 6-meV detuning case [Fig. 4(b)], the evolution with increasing intensity is less pronounced. For resonant or above resonant excitation, T_2 is always below our temporal resolution and we observe symmetric time dependences for all intensities. The $In_{1-x}Ga_xAs$/InP sample exhibits the same qualitative behavior.

III. THEORY OF TIME-RESOLVED FOUR-WAVE MIXING NEAR EXCITONIC RESONANCES

The optical response of semiconductors near the fundamental absorption edge is governed by excitonic effects. Nonlinearities are due to exciton-exciton interactions and anharmonicities in the exciton-photon interaction. Recently, following Ref. 7, theories based on the unrestricted Hartree-Fock (or BCS) approximation have been used successfully to describe coherent nonlinear-optical effects in semiconductors induced by excitation below, at, and above excitonic resonances.[7,8,14–18] In this section we derive the general expressions describing time-resolved FWM within the framework of the theory of Ref. 7. We discuss the salient features due to Coulomb interaction and present results of numerical calculations with parameters close to those of our experiments. We note that the

applicability of the noninteracting two-level model to time-resolved FWM in semiconductors has previously been criticized.[19]

We consider a parabolic two-band model with conduction band c and valence band v. Neglecting the photon momentum, the optically coupled conduction and valence band states form an inhomogeneous set of two-level systems labeled by wave vectors $\mathbf{k}$. The density matrix of the semiconductor breaks into 2×2 blocks,

$$\hat{n}_k(t)=\begin{bmatrix} n_{ck}(t) & \psi_k(t) \\ \psi_k^*(t) & n_{vk}(t) \end{bmatrix}, \tag{1}$$

where $n_{c,vk}$ are the populations in the conduction and valence bands, and ψ_k is the e-h pair amplitude. The density matrix obeys the Liouville equation ($\hbar=1$),

$$\frac{\partial}{\partial t}\hat{n}_k(t)=-i[\hat{\varepsilon}_k(t),\hat{n}_k(t)]+\frac{\partial}{\partial t}\hat{n}_k(t)|_{\text{relax}}, \tag{2}$$

where $\hat{\varepsilon}_k$ is the energy matrix. The difference between the BCS model of a semiconductor and a collection of noninteracting two-level systems is that the Coulomb interaction $V_{k,k'}$ couples the various states. In the presence of a "strong" pump field E, propagating in the direction $\mathbf{k}_2$, the energy matrix is

$$\hat{\varepsilon}_k(t)=\begin{bmatrix} \varepsilon_{ck}^0 & -\mu E(t) \\ -\mu^* E^*(t) & \varepsilon_{vk}^0 \end{bmatrix}-\sum_{\mathbf{k}'} V_{k,k'}\hat{n}_{k'}(t) . \tag{3}$$

μE is the Rabi frequency which describes the coupling of the two-level system at $\mathbf{k}$ to the pump field (in the dipole approximation). The unperturbed conduction and valence band energies are $\varepsilon_{ck}^0=E_g/2+k^2/2m_e$ and $\varepsilon_{vk}^0=-E_g/2-\mathbf{k}^2/2m_h+\sum_{\mathbf{k}'}V_{k,k'}$, where E_g is the band gap. As compared to noninteracting two-level systems, the physics is modified by the Coulomb force in two ways: (i) the conduction and valence band energies are renormalized,

$$\varepsilon_{jk}^0\rightarrow\varepsilon_{jk}(t)=\varepsilon_{jk}^0-\sum_{\mathbf{k}'}V_{k,k'}n_{jk'}(t),\quad j=c,v ; \tag{4a}$$

and (ii) the coupling to the light field is modified according to

$$\mu E(t)\rightarrow\Delta_k(t)=\mu E(t)+\sum_{\mathbf{k}'}V_{k,k'}\psi_{k'}(t) . \tag{4b}$$

This modification describes the fact that the optically coupled e-h states at $\mathbf{k}$ do not only experience the applied field μE; rather they see the self-consistent "local field" Δ_k, which is the sum of the applied field and the "molecular" field due to all the other e-h states at different wave vectors $\mathbf{k}'$.

The last term of Eq. (2) describes the coupling to the thermal reservoir and hence relaxation. For the purpose of the present discussion, we approximate this term by transverse and longitudinal relaxation rates $\gamma_2=T_2^{-1}$ and $\gamma_1=T_1^{-1}$, respectively. The temporal evolution of the e-h pair amplitude and the population is then given by

$$\left[\frac{\partial}{\partial t}+\gamma_2+i[\varepsilon_{ck}(t)-\varepsilon_{vk}(t)]\right]\psi_k(t)=i[1-2n_k(t)]\Delta_k(t) \tag{5a}$$

and

$$\left[\frac{\partial}{\partial t}+\gamma_1\right]n_k(t)=-i[\psi_k(t)\Delta_k^*(t)-\psi_k^*(t)\Delta_k(t)] , \tag{5b}$$

where we have used the e-h representation $n_{ck}\rightarrow n_k$ and $n_{vk}\rightarrow 1-n_k$.

In a FWM experiment a "weak" probe field δE, propagating in the direction $\mathbf{k}_1$, interferes with the pump field to generate a polarization propagating in the direction $\mathbf{k}_3=2\mathbf{k}_2-\mathbf{k}_1$. The linear response to the probe field is obtained by substituting $E\rightarrow E+\delta E$ in Eq. (2) and linearizing with respect to δE, which yields

$$\frac{\partial}{\partial t}\delta\hat{n}_k(t)=-i[\hat{\varepsilon}_k(t),\delta\hat{n}_k(t)]-i[\delta\hat{\varepsilon}_k(t),\hat{n}_k(t)]+\frac{\partial}{\partial t}\delta\hat{n}_k(t)|_{\text{relax}} , \tag{6}$$

where

$$\delta\hat{\varepsilon}_k(t)=\begin{bmatrix} 0 & -\mu\delta E(t) \\ -\mu^*\delta E^*(t) & 0 \end{bmatrix}-\sum_{\mathbf{k}'}V_{k,k'}\delta\hat{n}_{k'}(t) . \tag{7}$$

The change in the energy matrix $\delta\hat{\varepsilon}_k$ consists of two terms, the Rabi frequency associated with the probe field $\mu\delta E$ and the change in the molecular field $\sum_{\mathbf{k}'}V_{k,k'}\delta\hat{n}_{k'}$. The total polarization (per spin degree of freedom) induced by the probe field is

$$\delta P(t)=\sum_{\mathbf{k}}\mu^*\delta\psi_k(t) . \tag{8}$$

The FWM signal is given by the part $\delta P_{\mathbf{k}_3}$ of δP which propagates in the direction $\mathbf{k}_3$,

$$I_{\mathbf{k}_3}(T)\propto\int_{-\infty}^{\infty}dt|\delta P_{\mathbf{k}_3}(t)|^2 . \tag{9}$$

(The part $\delta P_{\mathbf{k}_1}$ of δP that propagates in the direction $\mathbf{k}_1$ describes the absorption and refraction of the probe beam as modified by the pump field.)

It is instructive to write explicitly the evolution equation for the probe-induced change in the e-h pair amplitude,

$$\left[\frac{\partial}{\partial t}+\gamma_2+i(\varepsilon_{ck}^0-\varepsilon_{vk}^0)\right]\delta\psi_k(t)-i\sum_{\mathbf{k}'}V_{k,k'}\delta\psi_{k'}(t)$$
$$=i[1-2n_k(t)]\mu\delta E(t)-i2\delta n_k(t)\mu E(t)-i2\sum_{\mathbf{k}'}V_{k,k'}[n_k(t)\delta\psi_{k'}(t)-n_{k'}(t)\delta\psi_k(t)+\delta n_k(t)\psi_{k'}(t)-\delta n_{k'}(t)\psi_k(t)] . \tag{10}$$

This is a driven time-dependent Wannier equation. In lowest order in the applied fields, where $n_k = \delta n_k = 0$, one recovers the form of the Wannier equation often used when nonlinear effects are neglected. The case of noninteracting *e-h* pairs is obtained be setting the Coulomb interaction $V_{k,k'}$ equal to zero. Then the above set of equations reduces to the usual Bloch equations for an inhomogeneously broadened two-level system.[1-3] This establishes a direct connection between the (BSC) density-matrix description of band-edge excitations and the more conventional theories of excitons in semiconductors and two-level systems. Let us note for the discussion of the forthcoming sections that in certain limiting cases and after some manipulations, Eqs. (5a) and (10) reduce to the equation of motion of a driven anharmonic oscillator (i.e., to a Ginzburg-Landau-like equation).[7] The driving terms in Eq. (10) deserve some comments. The first two contributions express the coupling to the applied fields corrected for Pauli exclusion. The Coulomb coupling, however, produces the third term, which is responsible for specific excitonic effects in the nonlinear response. This term comprises the so-called exciton-Hartree (proportional to n_k) and exciton-Fock (proportional to δn_k) terms.[7] As compared to the external field terms, these terms are proportional to the incoherent and coherent population (modulation) and the *e-h* pair amplitudes. Hence they have a very different temporal evolution. For example, in the case of excitation with ultrashort optical pulses, they exhibit a steplike onset and a subsequent decay, which is governed by the scattering rates γ_2 and γ_1. Since they are proportional to $V_{k,k'}$, they express exciton-exciton interactions and are thus absent for noninteracting two-level systems. It is also important to note that the diagonal interaction terms $\mathbf{k}=\mathbf{k}'$ vanish identically.

As we shall see, the above exciton-exciton interaction terms are most important to understand the behavior of the FWM signal at low and high intensities. In the case of noninteracting two-level systems $V_{k,k'}=0$, the dynamical response is well known.[3] It is depicted in Fig. 5 for the case of excitation with δ-shaped optical pulses (see also Sec. IV). In this figure we try to illustrate the physical processes involved in a FWM measurement. The optical pulses are indicated by the spikes, for clarity pulse 2 is represented larger. Along the horizontal time axis we plot the squared magnitude of the third-order polarization $|\delta P_{k_3}|^2$ for successive time delays T (light areas). The full area on the left time delay axis represents the time-integrated signal as measured by a slow detector. Clearly, there is no induced polarization for negative time delays (pulse 2 arrives before pulse 1). For positive time delays one finds an exponential decay of the polarization. The time constant of the decay of the time-integrated signal is $T_2/2$.[3]

To study the general case, we have solved numerically Eqs. (1)–(10) for parameters similar to those of our experiments. Following Ref. 7, we further decompose Eq. (10) into two coupled equations for the polarizations δP_{k_1} and δP_{k_3}, which are then directly integrated together with the equations for n_k, ψ_k, and δn_k. The latter quantity, which describes the grating formed by the pump and probe fields, is split into a part propagating in the direction $\mathbf{k}_1-\mathbf{k}_2$ and a (complex conjugate) part propagating in the direction $\mathbf{k}_2-\mathbf{k}_1$. Figure 6 shows the theoretical results for the diffracted signal, calculated for Gaussian pump and probe pulses of 110-fs duration tuned 3 rydbergs (Ry) below the exciton resonance. The material parameters are those of bulk GaAs and a dephasing time of $T_2=0.4\ \mathrm{Ry}^{-1}$ was assumed. Results for three different pump intensities are presented, corresponding to peak Rabi frequencies of 0.2, 0.6, and 0.8 Ry. They agree qualitatively with the experimental data. At low intensity (I_0), the time-integrated signal decays as expected with a time constant $T_2/2$ for positive time delay. For negative time delay, however, it exhibits a rising wing with a $T_2/4$ time constant. This has recently been verified experimentally in the case of a nearly homogeneous exciton line in GaAs QW's.[9] As the excitation intensity increases, the negative time delay signal becomes more pronounced ($9I_0$) and a temporal profile with two distinct maxima energies ($16I_0$), as seen in the case of

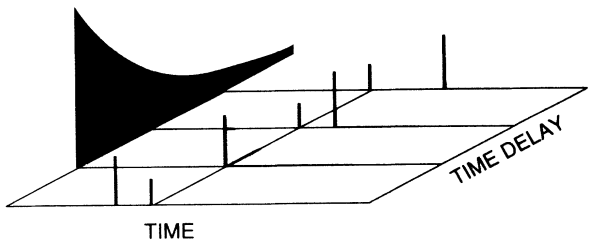

FIG. 5. Graphical representation of the predictions of the noninteracting two-level model of Ref. 3 for δ pulses. The temporal position of the two incident pulses is marked by the spikes. Pulse 2 is displayed with twice the strength of pulse 1. On the second line the two pulses overlap, which corresponds to zero time delay. The light areas represent the square of the magnitude of the third-order polarization as a function of time for various time delays. The full area on the left is the energy of the diffracted signal as a function of the time delay (i.e., the time integral of the light area at a given time delay).

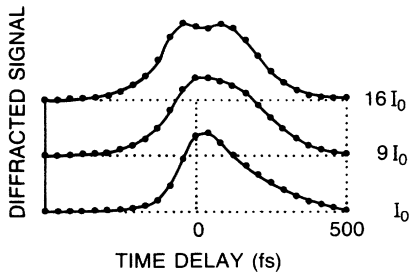

FIG. 6. Calculated diffracted signal vs time delay for three different excitation intensities. The points are the results of a numerical solution to all orders of the quantum kinetic equations for interacting excitons in semiconductors and qualitatively reproduce the data shown in Fig. 4(a).

$In_{1-x}Ga_xAs$ QW's [Fig. 4(a)]. The theory also reproduces the shoulder observed in Fig. 4(b) at small detuning.

The numerical solutions confirm that the unusual FWM time profile is due to the Coulomb interaction which mediates a nonlinear coupling of populations and pair amplitudes. Due to the complexity of the equations and the extreme time consumption of the numerical solution it is, however, difficult to follow the details of the mechanisms involved. In Secs. IV and V we discuss two idealized phenomenological models which are simple enough that they can be treated analytically and yet contain all the important physics.

IV. TIME-RESOLVED FOUR-WAVE MIXING IN A DENSE SYSTEM OF TWO-LEVEL ATOMS WITH LOCAL-FIELD CORRECTIONS

A system of interacting electrons and holes in the presence of an external field is somewhat analogous to a paramagnet or a dense dielectric medium. In both cases "local-field effects" are very important and in fact can dominate the physics. In this section we exploit this similarity and consider a dense medium consisting of interacting two-level atoms.[20] The atomic transition amplitude ψ and excited state population n satisfy the usual Bloch equations in which the driving terms involve not only the applied field E, but the Lorentz local field $E_{\rm loc}=E+LP$. Here, L is the Lorentz local field factor and $P=N\mu^*\psi$ is the polarization, where N is the density of atoms. The polarization and the excited state density $\nu=Nn$ obey the Bloch equations

$$\left[\frac{\partial}{\partial t}+\gamma_2+i(\varepsilon_1-\varepsilon_2)\right]P(t)=i[N-2\nu(t)]|\mu|^2E_{\rm loc}(t) \tag{11a}$$

and

$$\left[\frac{\partial}{\partial t}+\gamma_1\right]\nu(t)=-i[P(t)E^*_{\rm loc}(t)-P^*(t)E_{\rm loc}(t)] . \tag{11b}$$

These equations have the same structure as Eqs. (5), although as already noted the self-interaction term $k=k'$ vanishes in Eq. (5a). In linear response one finds that L merely renormalizes the transition energy to $\Omega=\varepsilon_1-\varepsilon_2-V$, where $V=N|\mu|^2L$.

The perturbation treatment of the Bloch equations (11) is similar to that without local-field corrections.[1-3] Up to third order, one finds

$$\left[\frac{\partial}{\partial t}+\gamma_2+i\Omega\right]P^{(1)}(t)=iN|\mu|^2E(t) , \tag{12a}$$

$$\left[\frac{\partial}{\partial t}+\gamma_1\right]\nu^{(2)}(t)=\left[\frac{\partial}{\partial t}+2\gamma_2\right]\frac{|P^{(1)}(t)|^2}{N|\mu|^2} , \tag{12b}$$

and

$$\left[\frac{\partial}{\partial t}+\gamma_1+i\Omega\right]P^{(3)}(t) =-i2|\mu|^2\nu^{(2)}(t)[E(t)+LP^{(1)}(t)] . \tag{12c}$$

As in Eq. (10), the driving term in Eq. (12c) consists of two types of contributions. The first one mixes the second-order excited-state density with the applied field, while the second one mixes it with the first-order polarization. This is the crucial difference between a noninteracting and an interacting set of two-level atoms. We consider the FWM situation where the applied field consists of two short pulses with a time delay T, i.e., $E\delta(t-T)\exp(i\mathbf{k}_2\cdot\mathbf{r})+\delta E\delta(t)\exp(i\mathbf{k}_1\cdot\mathbf{r})$. Solving Eqs. (12) yields for a homogeneously broadened system

$$\delta P^{(3),\rm hom}_{\mathbf{k}_3}(t)=\kappa e^{-i\Omega(t-2T)-\gamma_2 t}\{\Theta(T)\Theta(t-T)+i(2V/\gamma_1)[\Theta(T)\Theta(t-T)(1-e^{-\gamma_1(t-T)}) +\Theta(-T)\Theta(t)(1-e^{-\gamma_1 t})e^{2\gamma_2 T}]\} , \tag{13}$$

where $\kappa=-iN|\mu|^4E^2\delta E^*$ and Θ is the Heaviside step function. Equation (13) comprises three terms. The first one is the usual term for noninteracting two-level atoms, which contributes for positive time delay only [proportional to $\Theta(T)$].[3] The two other terms (proportional to V) are due to the local-field correction. The first one [proportional to $\Theta(T)$] also contributes at positive time delay whereas the other [proportional to $\Theta(-T)$] contributes only at negative time delay. It is interesting to note that the three terms are orthogonal. The first one is orthogonal in the complex plane to the two others, which are orthogonal to one another in time. Thus the three contributions do not interfere. The time-integrated diffracted signal is

$$I^{\rm hom}_{\mathbf{k}_3}(T)\propto\Theta(T)e^{-2\gamma_2 T}+\frac{4V^2}{(2\gamma_2+\gamma_1)(\gamma_2+\gamma_1)} \times[\Theta(T)e^{-2\gamma_2 T}+\Theta(-T)e^{4\gamma_2 T}] . \tag{14}$$

The signal exhibits a finite rise time with a time constant $T_2/4$ and a decay with a time constant $T_2/2$, as discussed for the case of exciton-exciton interactions [Fig. 7(a)].[8,9] It is now easy to interpret the results intuitively. With or without local-field interaction a grating is formed once both pulse 1 and pulse 2 (for either time ordering) have arrived in the sample. Without local-field interaction only the applied fields can diffract from this grating.

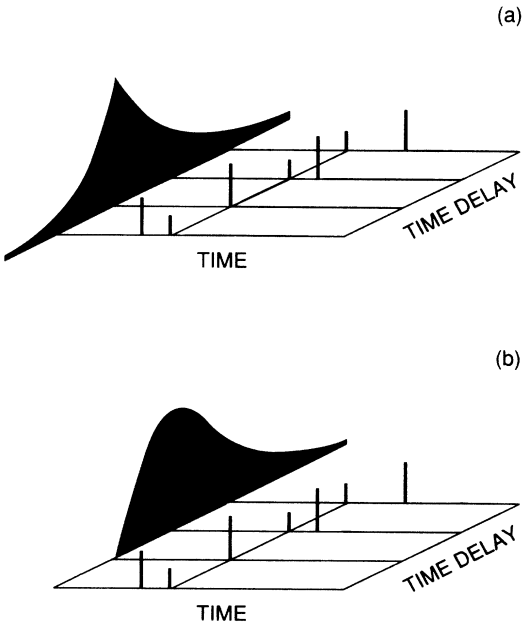

FIG. 7. Same as Fig. 5, but including local-field corrections. Results for (a) a homogeneously broadened line and (b) a strongly inhomogeneously broadened line are depicted. In contrast to the noninteracting two-level model, Fig. 5, one also finds a signal for negative time delay. This additional signal, however, is quite sensitive to inhomogeneous broadening and eventually disappears completely for a strongly inhomogeneously broadened line.

If pulse 2 comes first (negative time delay), the grating is only set up after pulse 1 arrives. At this time, however, no photon from pulse 2 is available since pulse 2 has already passed the sample. Thus in the direction $2\mathbf{k}_2-\mathbf{k}_1$ no signal is generated for negative time delay. With local-field interaction, however it is possible to diffract the leftover of the first-order polarization induced by pulse 2 off the grating formed as soon as pulse 1 arrives. Since two first-order polarizations from pulse 2 are involved in this process and both decay with a time constant T_2 until pulse 1 arrives, the signal decays with twice the time constant for negative time delay.

We can now incorporate inhomogeneous broadening with a normalized Gaussian distribution function

$$\rho(\Omega)=\frac{1}{\sqrt{\pi}\sigma}e^{-(\Omega-\Omega_0)^2/\sigma^2} . \tag{15}$$

We obtain

$$\delta P_{\mathbf{k}_3}^{(3),\mathrm{inhom}}(t)=e^{-\sigma^2(t-2T)^2/4}\delta P_{\mathbf{k}_3}^{(3),\mathrm{hom}}(t) , \tag{16}$$

with Ω replaced by Ω_0 in Eq. (13). For a very inhomogeneous line $\gamma_2\ll\sigma$, a photon-echo-like response of the polarization is found. In this case the time-integrated diffracted signal is given by

$$I_{\mathbf{k}_3}^{\mathrm{inhom}}(T)\propto\Theta(T)e^{-4\gamma_2 T}\left[1+\left[\frac{2V}{\gamma_1}\right]^2(1-e^{-\gamma_1 T})^2\right] . \tag{17}$$

The shape of the signal now contains information both on T_2 and T_1. The decay is eventually governed by $T_2/4$ like in the noninteracting two-level model [Fig. 7(b)]. The inhomogeneous case explains why no signal at negative time delay is observed in the low-intensity experiments on $In_{1-x}Ga_xAs$ QW's for which $\sigma\approx 4\gamma_2$.

V. TIME-RESOLVED FOUR-WAVE MIXING AND THE ANHARMONIC OSCILLATOR

In the preceding sections we have analyzed situations where a negative time delay signal is produced by collective effects. In this section we show that a single system can also exhibit such a behavior provided that the equation of motion comprises terms with the proper nonlinearity. The anharmonic oscillator is one of the standard models in nonlinear optics.[2] It is interesting to note that the kinetic equations for semiconductors can be arranged into the form of a harmonic oscillator with a nonlinear driving term[7] and the electronic transitions in large molecules are often modeled by an anharmonic potential. In Eq. (18) we add an arbitrary anharmonic potential $V(P)$ to the dynamics of the polarization P,

$$\left[\frac{\partial^2}{\partial t^2}+2\gamma_2\frac{\partial}{\partial t}+\Omega^2\right]P(t) = -\nabla_P V(P)(t)+\lambda[E(t)+E^*(t)] , \tag{18}$$

where $\lambda=2\Omega|\mu|^2$. We expand $V(P)$ in a power series

$$V(P)=\tfrac{1}{4}\alpha_3 P^4-\tfrac{1}{6}\alpha_5 P^6+\cdots . \tag{19}$$

Here we have assumed inversion symmetry of the problem and dropped the uneven terms. Again inhomogeneous broadening is accounted for by a Gaussian distribution. For the same δ-shaped pulses as in Sec. IV and for $\Omega_0\gg\gamma_2,\sigma$, we find the following general result up to fifth order:

$$\begin{aligned}\delta P_{\mathbf{k}_3}(t)=&\frac{A_3}{3}\{2\cos(\Omega_0 t)e^{-(1/4)\sigma^2 t^2}+\cos[\Omega_0(t-2T)]e^{-(1/4)\sigma^2(t-2T)^2}\}\\&\times[\Theta(T)\Theta(t-T)(e^{-\gamma_2(3t-2T)}-e^{-\gamma_2 t})+\Theta(-T)\Theta(t)(e^{-\gamma_2(3t-2T)}-e^{-\gamma_2(t-2T)})]\\&+\frac{A_5}{5}\{3\cos(\Omega_0 t)e^{-(1/4)\sigma^2 t^2}+2\cos[\Omega_0(t-2T)]e^{-(1/4)\sigma^2(t-2T)^2}\}\\&\times[\Theta(T)\Theta(t-T)(e^{-\gamma_2(5t-4T)}-e^{-\gamma_2 t})+\Theta(-T)\Theta(t)(e^{-\gamma_2(5t-4T)}-e^{-\gamma_2(t-4T)})] ,\end{aligned} \tag{20}$$

where A_3 and A_5 are given by

$$A_3 = -\tfrac{9}{16}\alpha_3\gamma_2^{-1}\Omega_0^{-4}\lambda^3 E^2\delta E^* ,$$

$$A_5 = \tfrac{25}{16}\alpha_5\gamma_2^{-1}\Omega_0^{-6}\lambda^5 E^3 E^*\delta E^* .$$

A_3 and A_5 reflect the strength of the third- and fifth-order terms, respectively. The homogeneous case is obtained by setting the inhomogeneous broadening σ equal to zero. The time-integrated diffracted signal for a homogeneous line and to third order is

$$I_{\mathbf{k}_3}^{\mathrm{hom}}(T) \propto \Theta(T)e^{-2\gamma_2 T} + \Theta(-T)e^{4\gamma_2 T} . \tag{21}$$

This dependence is shown in Fig. 8(a). The anharmonic oscillator displays the same exponential rise with $T_2/4$ for negative time delays as discussed in Sec. IV. For a strongly inhomogeneously broadened line $\gamma_2 \ll \sigma$, we find the signal

$$I_{\mathbf{k}_3}^{\mathrm{inhom}}(T) \propto \Theta(T)(e^{-8\gamma_2 T} - 2e^{-6\gamma_2 T} + e^{-4\gamma_2 T}) , \tag{22}$$

which decays with $T_2/4$ for large positive time delays and is identical to zero for negative time delays. Both the homogeneous and the inhomogeneous case are thus qualitatively similar to the local-field model discussed in Sec. IV. The regime for intermediate inhomogeneous broadening exhibits a narrow spike at $T=0$ that is related to the inverse bandwidth of the inhomogeneous broadening.

For a homogeneous line the time-integrated diffracted signal up to fifth order is

$$I_{\mathbf{k}_3}^{\mathrm{hom}}(T) \propto \Theta(T)\left[1 + \frac{A_5}{A_3}\frac{5}{2} + \frac{A_5^2}{A_3^2}\frac{8}{5}\right]e^{-2\gamma_2 T} + \Theta(-T)\left[e^{4\gamma_2 T} + \frac{A_5}{A_3}\frac{5}{2}e^{6\gamma_2 T} + \frac{A_5^2}{A_3^2}\frac{8}{5}e^{8\gamma_2 T}\right] . \tag{23}$$

The ratio A_5/A_3 is proportional to the intensity. We show one example for $A_5/A_3 = -0.9$ in Fig. 8(b) which illustrates the interference of the third- and fifth-order terms. From Eq. (23) we see that with increasing A_5/A_3 first the negative time delay signal gains relative strength (terms linear in A_5) until finally two distinct maxima appear (terms quadratic in A_5); see Fig. 8(b). This qualitatively describes the experimental findings at high intensities [Fig. 4(a)]. For large negative time delays the signal eventually decays with $T_2/4$.

Again the results can be understood quite intuitively. The fifth-order polarization has the opposite sign of the third-order polarization. Also, since one has to mix five first-order polarizations for the fifth-order polarization, it is expected to decay more rapidly in time. Thus we obtain a pronounced destructive interference close to zero time delay. The interference can very nicely be seen in the time-dependent polarization close to $T=0$ in Fig. 8(b). This destructive interference takes away energy from the time-integrated signal and thus leads to a minimum of the signal close to zero time delay. For a strongly inhomogeneously broadened line the signal for negative time delays is again identical to zero and no such interference is expected.

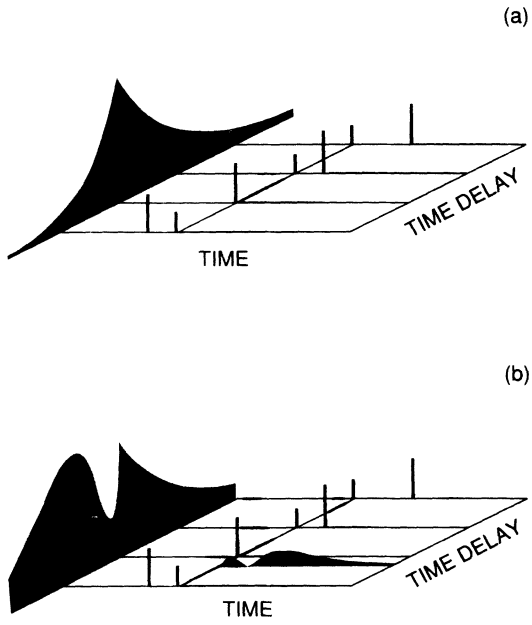

FIG. 8. Same as Fig. 5, but for an anharmonic oscillator. (a) shows the four-wave mixing response at low intensity, (b) at high intensity where also the fifth-order terms contribute. Around zero time delay, the latter interfere destructively with the third-order ones, which leads to the pronounced dip in the diffracted signal. Again, inhomogeneous broadening suppresses these effects.

VI. CONCLUSIONS

We have demonstrated both experimentally and theoretically that coherent polarization interactions lead to new nonlinear-optical effects in time-resolved four-wave mixing. These effects can be interpreted as due to scattering of the polarization off a polarization grating. At low intensities, this gives rise to a diffracted signal at negative time delays, with a time constant half that for positive time delays. At high intensities, a diffracted signal with two distinct temporal maxima evolves. Both effects vanish for strong inhomogeneous broadening.

Although discovered in the context of excitons in semiconductors, these phenomena are much more general and should be seen in many other systems. We have explicitly studied two-level systems with local-field corrections and the anharmonic oscillator. The former might describe a molecular crystal and the latter a large molecule, for instance.

ACKNOWLEDGMENTS

We would like to thank E. O. Göbel for stimulating some of this work. We are furthermore indebted to G. Sucha for his assistance with the color center laser, to S. Weiss and K. Leo for useful discussions, and to T. Chang, A. Cho, U. Koren, B. Miller, N. Sauer, and D. Sivco for providing the In-Ga-As samples.

[1]L. Allen and J. H. Eberly, *Optical Resonances and Two-Level Atoms* (Wiley, New York, 1975).

[2]Y. R. Shen, *The Principles of Nonlinear Optics* (Wiley, New York, 1984).

[3]T. Yajima and Y. Taira, J. Phys. Soc. Jpn. **47**, 1620 (1979).

[4]L. Schultheis, M. D. Sturge, and J. Hegarty, Appl. Phys. Lett. **47**, 995 (1985); L. Schultheis, J. Kuhl, A. Honold, and C. W. Tu, Phys. Rev. Lett. **57**, 1635 (1986); **57**, 1797 (1986); A. Honold, L. Schultheis, J. Kuhl, and C. W. Tu, Appl. Phys. Lett. **52**, 2105 (1988); Phys. Rev. B **40**, 6442 (1989).

[5]E. O. Göbel, K. Leo, T. C. Damen, J. Shah, S. Schmitt-Rink, W. Schäfer, J. F. Müller, and K. Köhler, Phys. Rev. Lett. **64**, 1801 (1990).

[6]P. C. Becker, H. L. Fragnito, C. H. Brito Cruz, R. L. Fork, J. E. Cunningham, J. E. Henry, and C. V. Shank, Phys. Rev. Lett. **61**, 1647 (1988).

[7]S. Schmitt-Rink and D. S. Chemla, Phys. Rev. Lett. **57**, 2752 (1986); S. Schmitt-Rink, D. S. Chemla, and H. Haug, Phys. Rev. B **37**, 941 (1988); S. Schmitt-Rink, D. S. Chemla, and D. A. B. Miller, Adv. Phys. **38**, 89 (1989).

[8]C. Stafford, S. Schmitt-Rink, and W. Schäfer, Phys. Rev. B **41**, 10000 (1990).

[9]K. Leo, M. Wegener, J. Shah, D. S. Chemla, E. O. Göbel, T. C. Damen, S. Schmitt-Rink, and W. Schäfer, Phys. Rev. Lett. **65**, 1340 (1990).

[10]J. Mark, L. Y. Liu, H. A. Haus, and E. P. Ippen, Opt. Lett. **14**, 48 (1989).

[11]M. Wegener, I. Bar-Joseph, G. Sucha, M. N. Islam, N. Sauer, T. Y. Chang, and D. S. Chemla, Phys. Rev. B **39**, 12 794 (1988).

[12]M. S. Skolnick, P. R. Tapster, S. J. Bass, A. D. Pitt, N. Apsley, and S. P. Aldred, Semicond. Sci. Technol. **1**, 29 (1986).

[13]J. Feldmann, G. Peter, E. O. Göbel, P. Dawson, K. Moore, C. Foxon, and R. J. Elliott, Phys. Rev. Lett. **59**, 2337 (1987).

[14]W. Schäfer, Adv. Solid State Phys. **28**, 63 (1988); W. Schäfer, K. H. Schuldt, and R. Binder, Phys. Status Solidi B **150**, 407 (1988).

[15]C. Ell, J. F. Müller, K. El Sayed, L. Banyai, and H. Haug, Phys. Status Solidi B **150**, 393 (1988); C. Ell, J. F. Müller, K. El Sayed, and H. Haug, Phys. Rev. Lett. **62**, 304 (1989).

[16]R. Zimmermann, Phys. Status Solidi B **146**, 545 (1988); R. Zimmermann and M. Hartmann, *ibid.* **150**, 365 (1988).

[17]I. Balslev, R. Zimmermann, and A. Stahl, Phys. Rev. B **40**, 4095 (1989).

[18]R. Binder, S. W. Koch, M. Lindberg, N. Peyghambarian, and W. Schäfer, Phys. Rev. Lett. **65**, 899 (1990).

[19]I. Abram, Phys. Rev. B **40**, 5460 (1989).

[20]S. Mukamel, Z. Deng, and J. Grad, J. Opt. Soc. Am. B **5**, 804 (1988).

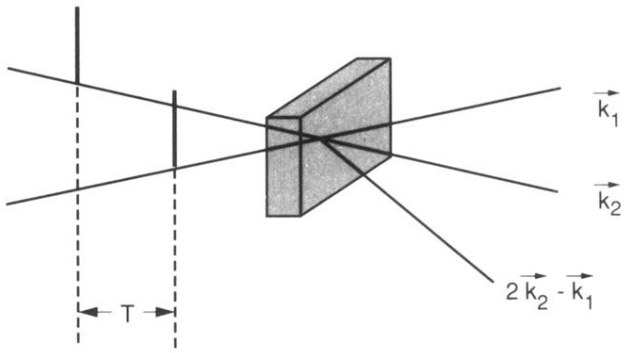

FIG. 1. Schematic of the geometry of four-wave mixing. In our notation, positive time delay T corresponds to pulse 1 preceding pulse 2.